Bioactive Materials 2 (2017) 19–26

Contents lists available at ScienceDirect

Bioactive Materials

journal homepage: http://www.keaipublishing.com/en/journals/bioactive-materials/

Effect of heat treatment on mechanical and biodegradable properties of an extruded ZK60 alloy

Junxiu Chen, Lili Tan, Ke Yang*

Institute of Metal Research, Chinese Academy of Sciences, 72 Wenhua Road, Shenyang 110016, China

ARTICLE INFO

Article history:
Received 29 January 2016
Received in revised form
11 December 2016
Accepted 12 December 2016
Available online 21 December 2016

Keywords:
ZK60 alloy
Heat treatment
Second phase
Corrosion

ABSTRACT

ZK60 magnesium alloy possess good mechanical properties and is a potential biodegradable material. But its high degradation rate is not desirable. In this study the effect of heat treatment on the biodegradable property of ZK60 alloy was investigated. T5 treated, T6 treated, as-cast and as-extruded ZK60 alloys were studied. Microstructure characterization, electrochemical measurement and immersion test were carried out. The results showed that both the mechanical properties and degradation behavior were improved after T5 treatment due to the formation of small and uniformly distributed MgZn phases. The as-cast alloys also exhibited good corrosion resistance. However, the as-extruded and T6 treated samples were severely corroded due to the formation of large amounts of second phases accelerating the corrosion rate owing to the galvanic corrosion. The corrosion resistance of ZK60 alloy was as following: T5 treated > as-cast > T6 treated > as-extruded.

1. Introduction

Magnesium (Mg) and its alloys as a new type of biodegradable materials have attracted good attentions of researchers, because of their good mechanical properties, such as density (1.7–2.0 g/cm^3) and Young's modulus (41–45 GPa), which are very close to human bones (1.8–2.1 g/cm^3) [1,2] and can diminish the "stress-shielding effect" [3]. The existent metal implants such as titanium alloys, stainless steel and cobalt-chromium alloys in the human body may cause allergic and sensitization [4]. Polymer material such as polyL-lactic acid owing to its low mechanical properties has limited its applications for biodegradable implants [5]. Magnesium is present naturally in bone tissues and can promote the growth of new bone tissue and bone metabolism [1,6,7]. However, one of the reasons why these new biomaterials have not been widely used is that their corrosion rate, or degradation rate, is high in physiological environments. Thus before the new bone tissue is healed they have already biodegraded [8]. The metallic ions through the rapid corrosion may lead to inflammatory cascades and reduce biocompatibility, what is more, rapid corrosion of magnesium releases more hydrogen gas, which is adverse to the tissue and more hydrogen gas leads to gas cysts. The tissues and the materials are separated by gas cyst delaying the bone healing [1]. Therefore it is necessary to improve its corrosion properties before we use it in clinical applications [9]. Though at present magnesium alloys are believed to be only used as unload-bearing implants, in some cases, magnesium alloys are developed to be used as screws whose mechanical property is still important to avoid the fracture during the implantation of the screw into the bone. ZK60 is a commercial magnesium alloy, a Mg-Zn-Zr alloy, with higher strength and elongation can meet this demand for mechanical properties [10]. Zinc (Zn) is an essential element in human body and is crucial for many biological functions [3]. Moreover, Zn can increase the age hardening response and refine the grain size of magnesium alloys [11,12]. It can also diminish the harmful effect causing by Fe impurities to improve the corrosion resistance [13]. However, the high degradation rate of ZK60 alloy (11.82μA/cm^2) is undesirable [14]. Many researchers applied different methods in order to further improve its corrosion resistance. Lin X et al. [14] fabricated a forsterite-containing micro-arc oxidation coating on ZK60 alloy, and the corrosion current densities of MAO-treated samples were at least one order of magnitude lower than that of the untreated ZK60 sample. However the biodegradation property of ZK60 substrate still has important effect on that of the coated ZK60. By adding RE element Nd into Mg-

* Corresponding author. Tel.: +86 024 23971628.
E-mail address: kyang@imr.ac.cn (K. Yang).
Peer review under responsibility of KeAi Communications Co., Ltd.

http://dx.doi.org/10.1016/j.bioactmat.2016.12.002

Zn-Zr, Yang Z et al. [15] explored a new alloy which had excellent corrosion resistance. However the long term biocompatibility of Nd needs to be studied to prove its bio-safety. In this work, we attempted to improve the corrosion resistance of ZK60 alloy by proper heat treatment through controlling the microstructure, studied the effect of heat treatment (T5 and T6 treatments) on the biodegradable property of an extruded ZK60 alloy, and analyzed the relevant biodegradation mechanism.

2. Experimental

The composition of ZK 60 alloy analyzed by ICP is listed in Table 1. The alloy was supplied by Institute of Metal Research, Chinese Academy of Sciences. ZK60 alloy ingots were heat treated at 400 °C for 12 h and then extruded. The extrusion process was as following: extrusion temperature was 390°C and extrusion ratio was 59. The materials diameters prior and after extrusion were 90 mm and 12 mm, respectively. After extrusion, the specimens were heat treated at 170 °C × 10 h (T5) and 500 °C × 2 + air cooling+170 °C × 10 h (T6), respectively. Four kinds of samples, namely, T5 treated, T6 treated, as-cast and as-extruded alloys were studied. The microstructures of ZK60 were observed. The samples were prepared by standard metallographic techniques and were etched in a solution containing 6 g picric, 10 ml acetic, 10 ml water and 70 ml ethanol. Standard specimens (M10 Φ5) were machined for tensile tests. The tensile tests were performed by using an Instron-5569 universal testing machine at a displacement rate of 1.0 mm/min at ambient temperature. Three specimens were tested for each group. Specimens with a surface area of 1.1304 cm^2 (diameter 12 mm) were molded in epoxy resin for electrochemical tests. The test was performed at 37 °C in Hank's solution at pH 7.4 by using PARSTAT 2263 potentiostat/galvanostat (Princeton Applied Research). A three-electrode cell was used for potentiodynamic polarization tests after 1800s stable time. saturated calomel electrode was use as a reference electrode with platinum electrode as a counter and was used as a the working electrode. The EIS experiments were performed at the open circuit potential with a frequency range of 10^5–0.1 Hz. Potentiodynamic polarization experiments were carried out with a scan rate of 0.5 mV/s initiated at −250 mV below the open-circuit potential (OPC). Specimens with a diameter of 12 mm and a height of 2 mm were immersed in Hank's solution [15]for 14 days. The ratio of specimen surface area (cm^2) to solution volume (mL) was 1.25. In order to keep the solution fresh, the solution was changed every day. The pH value was kept for 14 days. After immersion, the specimens were cleaned in a solution of chromium trioxide to remove the surface product and corrosion rate was calculated. Finally, the corrosion morphologies of the samples were observed by camera and SEM. Each experiment was repeated three times.

Table 1
The composition of experimental ZK60 alloy (wt.%).

Al	Zn	Mn	Fe	Ni	Zr	Si	Cu
<0.01	5.20	0.030	<0.01	<0.01	0.380	<0.01	<0.01

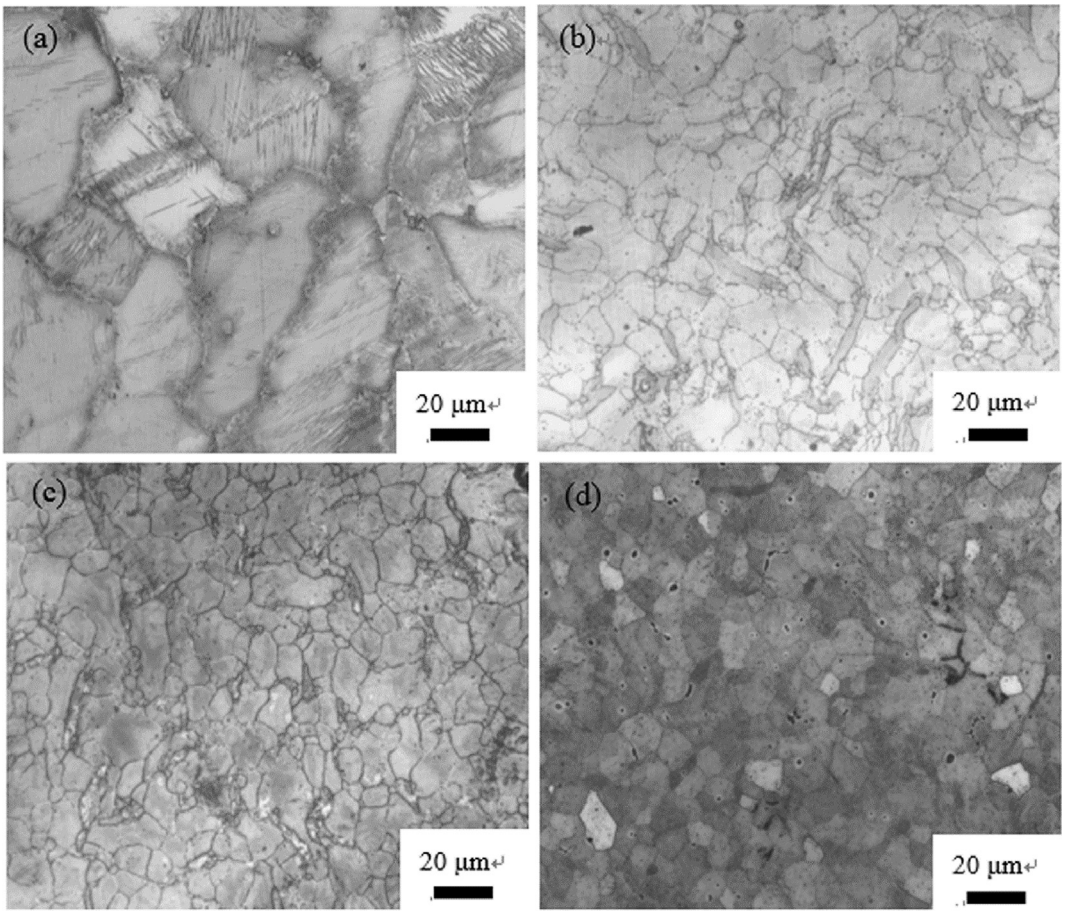

Fig. 1. The optical microstructure of ZK60 alloy (a) as-cast, (b) as-extruded, (c) T5 treated and (d) T6 treated.

3. Results and discussion

3.1. Microstructure and mechanical properties

The optical microstructures of ZK60 alloy are shown in Fig. 1. It can be seen that after extrusion the grain size of the alloy was drastically decreased from about 60 μm to about 10 μm.Therefore, grain refinement effect of extrusion is obvious. However, the grain size is not uniform and there are some small grains distributing between two larger grains. The small grain may be formed due to the recrystallization during extrusion. After T5 treatment, the grain size has no obvious change. But after T6 treatment, the grain size is more uniform due to the recrystallization completed. The SEM micrographs and EDS of ZK60 alloy are shown in Fig. 2. It can be seen that there are many second phases on the grain boundary. The size of second phase of the as-cast is the largest and the distribution of the second phase is concentrated, indicating that pitting corrosion is easy to happen in these areas. The main compositions of the second phase are α-Mg + MgZn intermetallics. After extrusion, the content of ZnZr phase is high in the second phase, some residue stress is exist due to work-hardening and amount of second phases are not uniform. All of the factor can decline the corrosion resistance. However, the content of the second phase MgZn intermetallics along the boundaries in T5 treated sample is more uniform than the other three, indicating a good corrosion resistance. In order to identify the composition of the extruded alloy after heat treatment, XRD analysis was carried out. From the Fig. 3, it can be seen that the main phases are $MgZn_2$ intermetallic. The results are consistent with SEM analysis. $MgZn_2$ phases are harmful to the corrosion resistance of ZK60 alloy due to the formation of galvanic corrosion. Fig. 4 shows the precipitation process. SSS is the supersaturation solution state. At the early aging stage, G.P. zone which is continuous with disk shape precipitated from the matrix along $\{0001\}_{Mg}$. At the middle aging stage, $MgZn_2$ phase which is also continuous with rod-like shape precipitated from the matrix-perpendicular to $\{0001\}_{Mg}$. At this state, the alloy had the best mechanical properties. With the increase of time, $MgZn_2$ phases grew up and were semicontinuous with disk shape and along $\{0001\}_{Mg}$. At the later aging stage, Mg_2Zn_3 phase which is uncontinuous with triangular shape precipitated. At this state, the mechanical properties of the alloy decreased drastically [16]. However, according to the XRD patterns, Mg_2Zn_3 phase are not detected.

It has been investigated that the strength of as-cast Mg-Zn alloys increases with the increase of Zn content until 5 wt%. However, the elongation decreases with the increase of Zn content [17]. When the content of Zn is over 5 wt%, many MgZn phases will precipitate from Mg matrix along grain boundaries, which can enhance the strength of Mg-Zn alloy due to the disperse strengthening

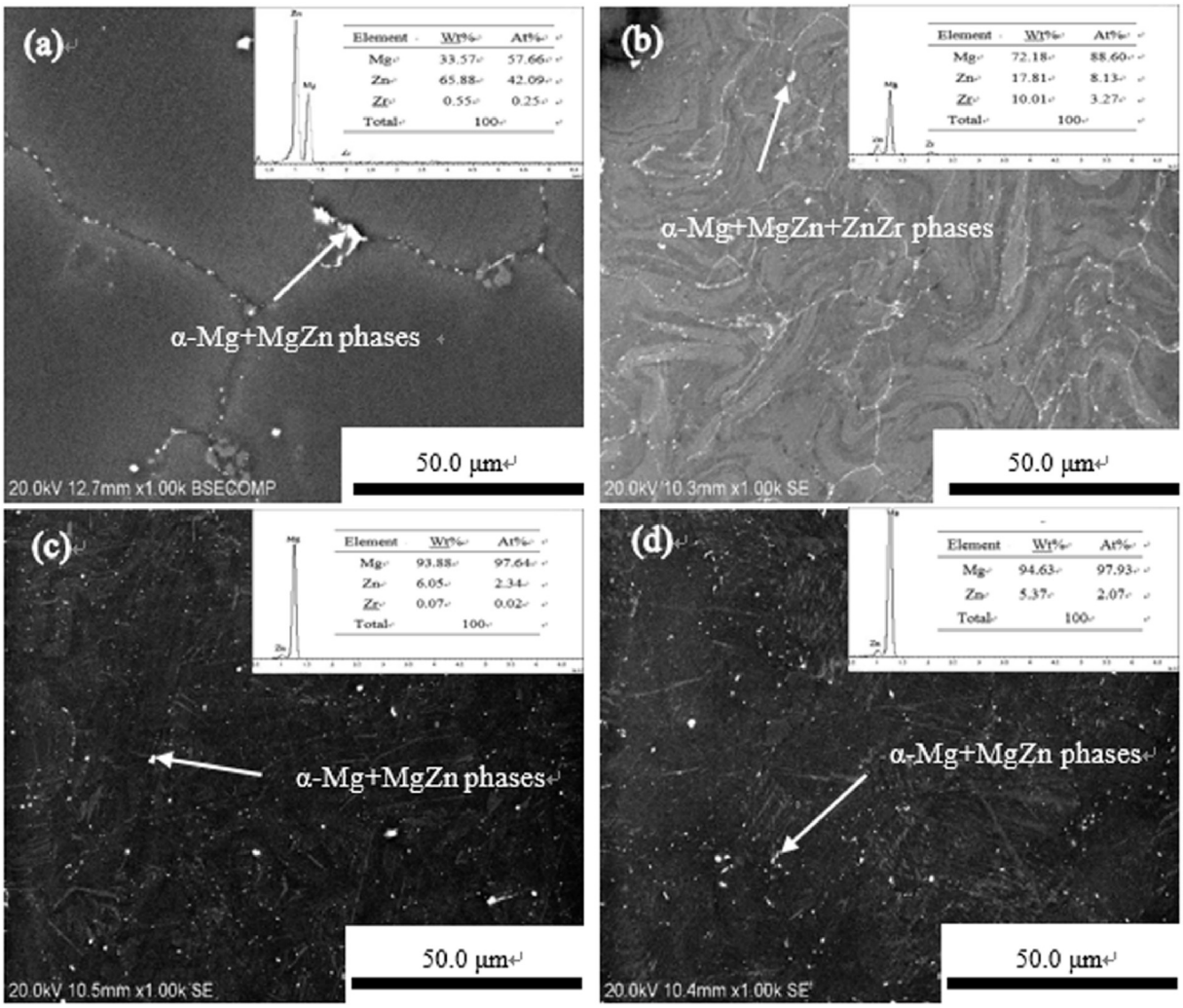

Fig. 2. SEM micrographs of ZK60 alloy (a) as-cast, (b) as-extruded, (c) T5 treated and (d) T6 treated.

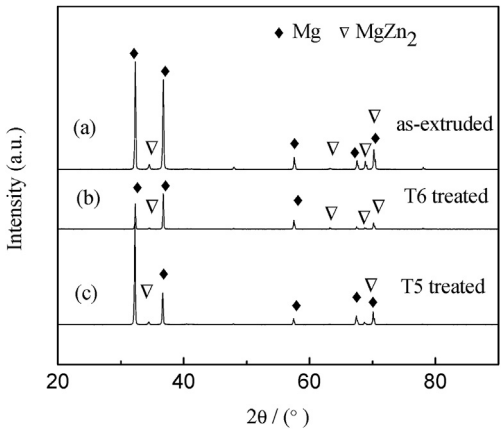

Fig. 3. X-ray diffraction patterns of extruded ZK60 (a) as-extruded, (b) T6 treated and (c) T5 treated.

mechanism [18]. The mechanical properties of ZK60 can be improved after extrusion and after T5 treatment, the $MgZn_2$ phase precipitated along the grain boundary, with small size and uniform distribution. They were either continuous or semi continuous with the matrix, leading to the formation of elastic distortion in the alloy. This elastic strain fields could inhibit the dislocation motion and result in the strengthening effect, but decrease the ductility. Especially, when they are continuous, the elastic strain fields will be cohesive, and the strengthening effect is the most significant [19]. After T6 treatment, because of the solid solution at high temperature, the grain size of the matrix was large and the MgZn phases precipitated on the grain boundary were thick, coarse and not uniform. Thus, there would be some crack resources on the grain boundaries resulting in strength shrinkage. However, high temperature solid solution can eliminate the work-hardening and residual stress, resulting in the improvement of ductility. The mechanical properties of the three states of ZK60 alloy are listed in Table 2. It can be seen obviously that T5 treated samples not only exhibit good yield strength and tensile strength but also shows good ductility.

3.2. Electrochemical measurements

The standard potential of magnesium is −2.37 V at 25 °C with strong electro negativity and the standard potential of Zn is −0.762 V [20]. A Mg-Zn alloy was easily corroded due to the formation of galvanic battery. $MgZn_2$ phase acts as cathode and Mg matrix acts as anode. If $MgZn_2$ phase are fine and continuous, the corrosion rate can be decreased. The as-cast Mg-Zn alloy can form a protective film on the surface of alloy in simulated body fluid (SBF). It was reported that Mg-5Zn alloy exhibited the best corrosion resistance [17]. Fig. 5 shows the potentiodynamic polarization curves of the four states of alloy and Table 3 is the result of Tafel fitting. It can be seen that the T5 heat treated alloy exhibited the best corrosion resistance with the lowest corrosion current (5.31 μA/cm^2). The corrosion current density, i_{corr} (μA/cm^2), is related to the corrosion rate, P_i with using the following equation [21].

$$P_i = 22.85 i_{corr} \quad (1)$$

According to the current density, the corrosion resistance can be ranked as following: T treated > as-cast > T6 treated > as-extruded. For magnesium alloys, the degradation reactions in Hank's solution are presented by the following equations [3,21,22]:

Table 2
Mechanical properties of the three states of ZK60.

Specimens	Yield strength (MPa)	Tensile strength (MPa)	Elongation (%)
As-extruded	210 ± 10.80	300 ± 0.42	19.6 ± 0.73
T5 treated	274 ± 5.83	324 ± 1.57	17.9 ± 1.07
T6 treated	202 ± 2.50	289 ± 0.42	23.2 ± 1.05

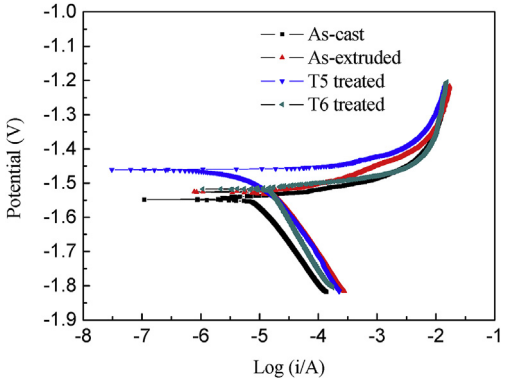

Fig. 5. Potentiodynamic polarization curves of the three states of ZK60 with a scan rate of 0.5 mV/s in Hank's solution at 37 °C.

Table 3
The Tafel fitting results based on potentiodynamic polarization tested in Hank's solution (i_{corr} represented the corrosion current and E_{corr} represented the corrosion potential).

Specimens	i_{corr} (μA/cm^2)	E_{corr}(v) vs. SCE	Corrosion rate (mm/y)
As-extruded	21.60 ± 1.10	−1.51 ± 0.018	0.494 ± 0.0025
As-cast	8.96 ± 0.82	−1.53 ± 0.015	0.247 ± 0.0019
T5 treated	5.31 ± 0.40	−1.48 ± 0.015	0.12 ± 0.0009
T6 treated	17.17 ± 1.74	−1.520 ± 0.002	0.485 ± 0.0040

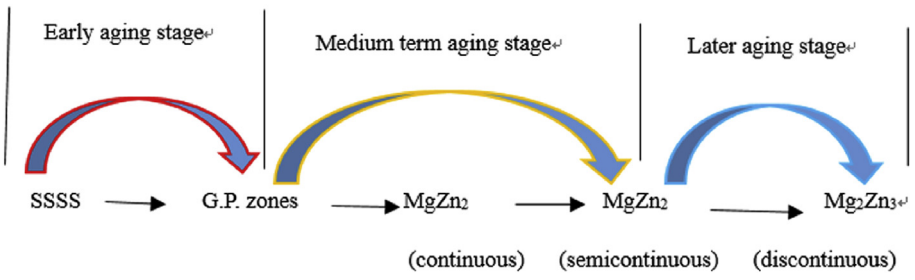

Fig. 4. The sketch of the age-precipitated phases formation in ZK60 alloy.

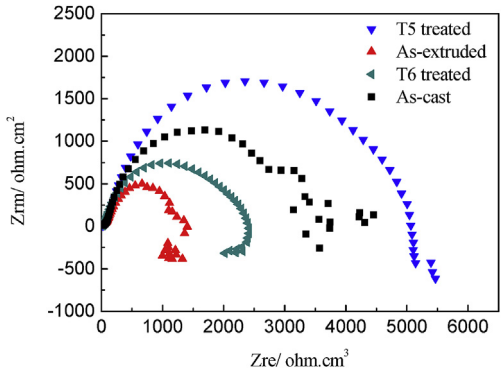

Fig. 6. EIS curves of the three states of ZK60 at the open circuit potential with the frequency range of 10^5–0.1 Hz in Hank's solution at 37 °C.

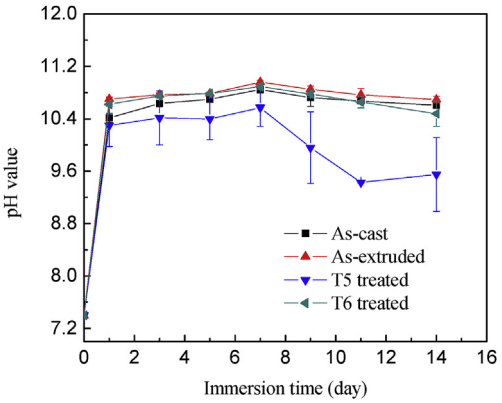

Fig. 9. pH values at different times for the three states of alloy in Hank's solution.

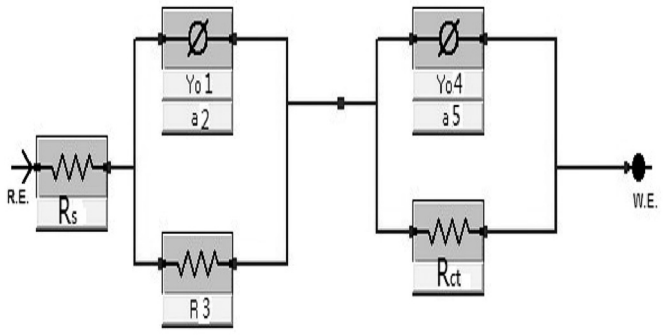

Fig. 7. Equivalent circuit of T5 treated and as-cast ZK60 in Hank's solution at 37 °C.

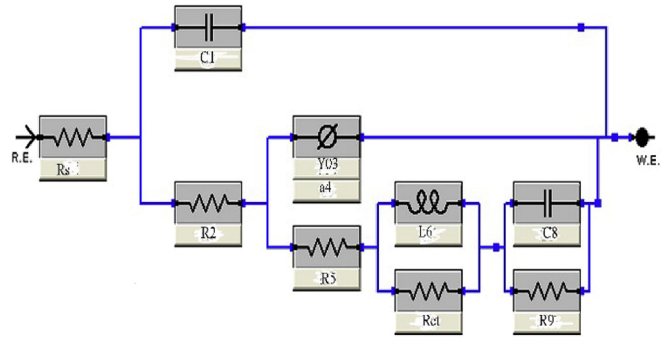

Fig. 8. Equivalent circuit of as-extruded and T6 treated ZK60 in Hank's solution at 37 °C.

Table 4
Fitting results of T5, T6 treated and as-cast ZK60 alloys immersed in Hank's solution.

Specimens	R_s (Ω)	Y_01 (S·sec^n)	a2	R3 (Ω)	Y_04 (S· sec^n)	a5	R_{ct} (Ω)
T5 treated	21.23	1.727e-5	0.7	83.81	2.44 e-5	0.8	4.968 e3
As-cast	8.722	1.935e-5	0.9	2901	1.25e-3	0.3	3.195e3

$$Mg \rightarrow Mg^{2+} + 2e^- \quad (2)$$

$$2H_2O + 2e^- \rightarrow H_2 + 2OH^- \quad (3)$$

$$Mg^{2+} + 2OH^- \leftrightarrow Mg(OH)_2 \quad (4)$$

$$Mg^{2+} + 2Cl^- \leftrightarrow MgCl_2 \quad (5)$$

The surface product $Mg(OH)_2$ is not compact, allow the solution particle to penetrate through easily. The magnesium alloys will corrode steadily due to the existence of chloride ions [23]. This corrosion mechanism exists for all the magnesium alloys. The second phase plays dual roles in the corrosion behavior, i.e., the finely and continuously distributed second phase can effectively decrease the corrosion rate, otherwise, will accelerate the corrosion process [15,24]. The corrosion of ZK60 is closely related to the galvanic corrosion, the second phase MgZn phase and Zn-Zr phase acting as micro-cathode has a great effect on the corrosion. After T5 heat treatment, the MgZn intermetallic phase was small, uniform and more continuously distributed than those in the other three states of alloy, which could reduce the galvanic corrosion effect. The alloy after T5 heat treatment exhibited the best corrosion resistance. After T6 heat treatment, much MgZn phases precipitated along the grain boundary to form galvanic corrosion. The galvanic effect increased the corrosion rate drastically, exhibiting the decrement of corrosion resistance. There were more Zr-rich phases (ZnZr) in as-extruded ZK60 and residue stress was exist due to work-hardening. Besides, the composition was not uniform without heat treatment. Thus, the as-extruded ZK60 had the worst corrosion resistance. The as-cast ZK60 had no more second phases than the as-extruded and T6 treated alloys also exhibiting good corrosion resistance.

The electrochemical impedance spectroscopy (EIS) is a useful method to analyze the electrochemical corrosion of metals. The EIS curves and the fitted curves of the three states of ZK60 alloy are displayed in Fig. 6. One capacitive loop and one inductance loop are observed on the Nyquist plot of the as-extruded and T6 treated

Table 5
Fitting results of as-extruded ZK60 alloys immersed in Hank's solution.

Specimens	R_s (Ω)	C1 (F)	R2 (Ω)	Y_03 (S· sec^n)	a4	R_5 (Ω)	L6 (H)	R_{ct} (Ω)	C8 (F)	R9 (Ω)
As-extruded	19.85	4.28E-7	51.83	2.64 E-5	0.8	2.22e-3	9873	1296	5.02E-9	9.48E-4
T6 treated	20.43	7.18E-7	28.78	3.51E-5	0.8	0.023	3.86E-9	2271	1.26E-13	1.04E-3

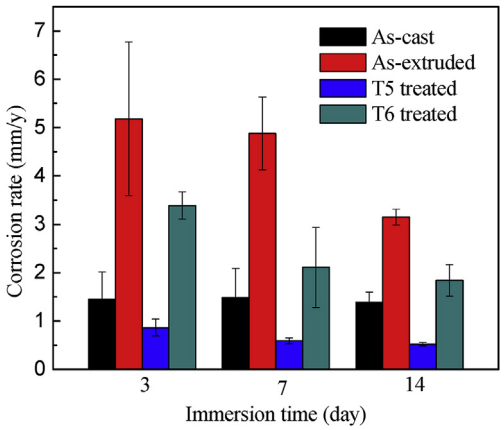

Fig. 10. The corrosion rate of the three states of alloy after immersing in Hank's solution for 14 days.

ZK60 alloy at high frequency and low frequency, respectively. For the as-cast and T5 treated ZK60 alloys, the EIS curves exhibit mainly single capacitive loops. It was found that the diameter of the capacitive loop of T5 treated ZK60 was larger than the as-cast ZK60. What's more, the diameter of the capacitive loop of T5 treated ZK60 was the largest among the four curves. The high frequency behavior of EIS is associated with corrosion rate. The relation between the diameter of high frequency capacitive loop and corrosion rate of magnesium has been verified [25]. The larger diameter of high frequency mean's good corrosion resistance. It can be concluded that T5 treated ZK60 with the largest diameter of high frequency capacitive loop has the best corrosion resistance. So the corrosion resistance can be ranked as following: T5 treated > as-cast > T6 treated > as-extruded. Finally, the low frequency inductive loop implies the occurrence of pitting corrosion on the as-extruded and T6 treated ZK60 [26].

The equivalent circuit models for the EIS curves and the fitting results are presented in Figs. 7 and 8, Tables 4 and 5, respectively. The data were fitted by ZSimpWin software. In Fig. 7, the first part ($Y_0$1, a2, R_3) represents the electric double layer capacitance at the interface of the degradation products and electrolyte. The second part ($Y_0$4, a5, R_{ct}) represents the electric double layer capacitance at the interface of the ZK60 alloy and electrolyte. In Fig. 8, L6 indicate the existence of metastable Mg^{2+} during dissolution of the ZK60 alloy. The charge transfer R_{ct} is a parameter that is closely related to the corrosion resistance of the material. The larger value of R_{ct} represents high corrosion resistant materials. R_{ct} of T5 treated ZK60 (4968 Ω) is much larger than the other three states of alloy (3195Ω, 2271 Ω and 1296 Ω), implying that the electrochemical reaction was hindered effectively on the surface between the sample and electrolyte. According to the values of R_{ct}, the corrosion resistance of the three states of ZK60 was ranked as following: T5 treated alloys > as-cast > T6 treated > as-extruded. This result is consistent with that of potentiodynamic polarization measurement.

3.3. Immersion test

The *in vitro* degradation of the extruded samples was evaluated in Hank's solution. Fig. 9 shows the variation of pH value of solution as a function of immersion time. It can be seen that pH values of the four states of ZK60 alloy increase with the time. However, the pH value of T5 treated alloy increases lag behind the other three states of alloy. Fig. 10 shows the corrosion rate after immersing for 14 days. The corrosion rates (P_i, mm/y) are given below:

$$P_i = (K \times W)/(A \times T \times D) \quad (6)$$

where the coefficient $K = 8.76 \times 10^4$, W is the weight loss(g), A is the sample area exposed to solution (cm^2), T is the exposure time (h) and D is the density of the material (g/cm^3).

Fig. 10 shows that the corrosion rate of the as-cast, as-extruded, T5 treated and T6 treated ZK60 alloys, which was in the following

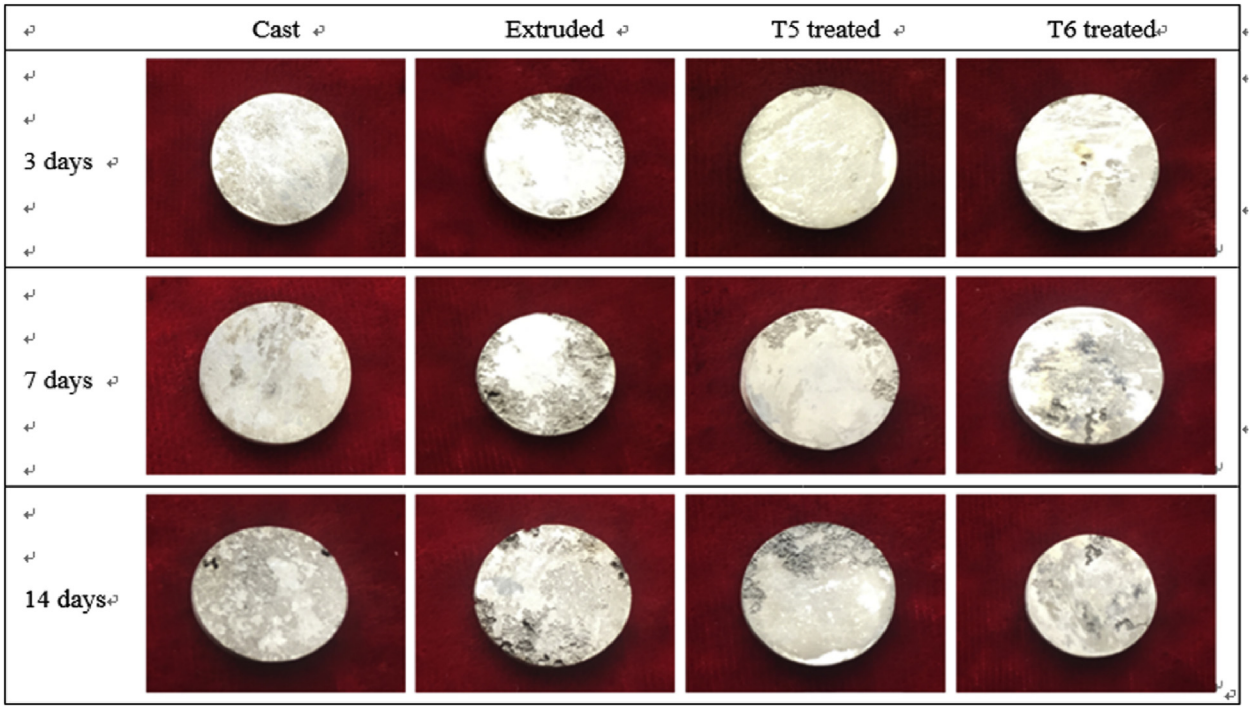

Fig. 11. Macroscopic of ZK60 alloy after immersion different times (3 days, 7 days and 14 days) in Hank's solution and rinsed with chromic acid.

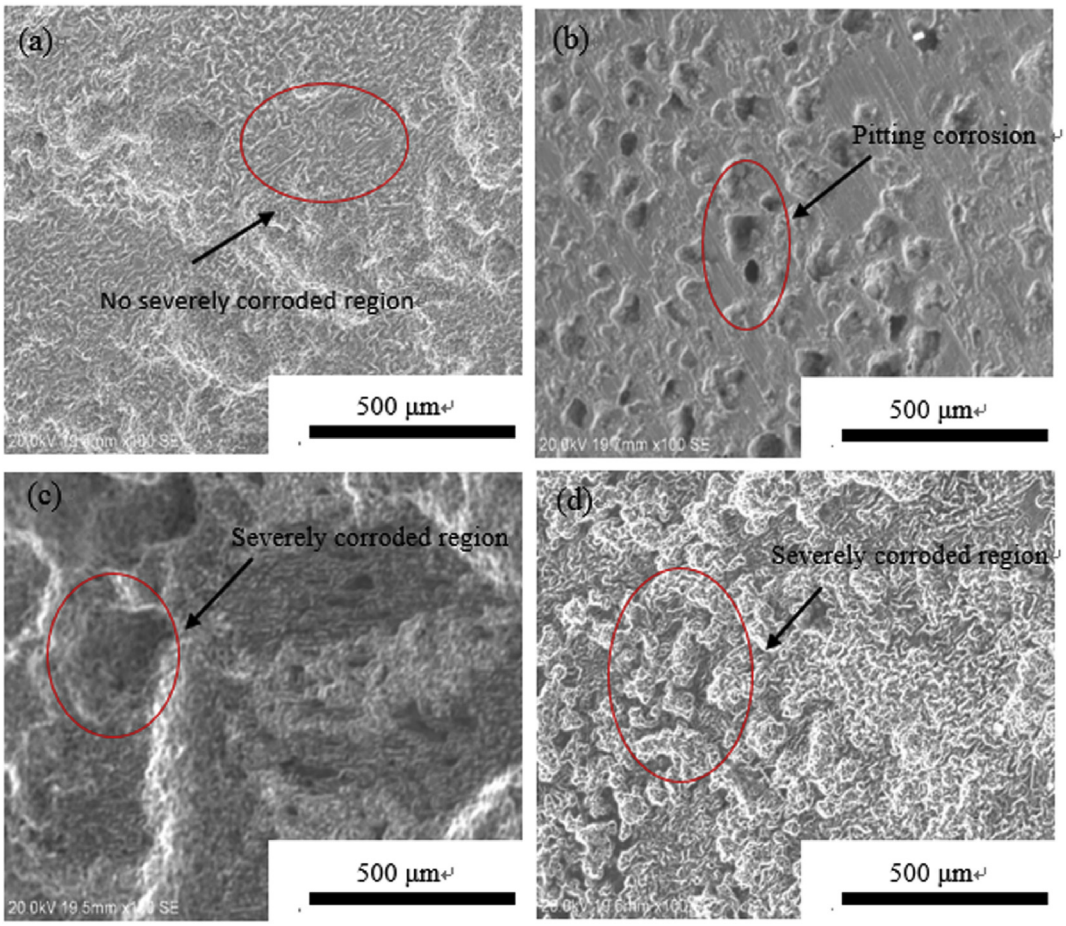

Fig. 12. The SEM images of the alloys immersed in Hank's solution after 14 days: (a) T5 treated (b) As-cast (c) T6 treated (d) as-extruded.

order: T5 treated > as-cast > T6 treated > as-extruded. Pitting corrosion is very common in magnesium alloys, which is caused by galvanic corrosion between the matrix and second phases [27]. The corrosion resistance of Mg-Li-Ca in Hank's solution was improved due to the fine-grained microstructure transferring the corrosion form from pitting corrosion to the general corrosion [28]. The corrosion morphology of T5 treated alloy also exhibits general corrosion. Figs. 11 and 12 show the macroscopic and microscopic morphologies of ZK60 after different immersion times, respectively. It can be seen that the alloys are mainly corroded by pitting corrosion and was found that as-extruded and T6 treated samples are severely corroded. Though the as-cast alloy is corroded by pitting corrosion, it shows good corrosion resistance compared with the as-extruded and T6 treated. Among them, T5 treated sample exhibits the best corrosion resistance.

4. Conclusion

In this work, we investigated the effect of heat treatment on the biodegradation of the extruded ZK60 alloy. T5 treated, T6 treated, as-cast and as-extruded ZK60 alloys were studied. The conclusion could be obtained as following:

(1) The alloy after T5 treatment presented small and uniform second phases distribution, exhibiting good mechanical properties and corrosion resistance. However, the as-extruded ZK60 exhibited the worst corrosion resistance. The content of ZnZr phase is high in the second phase and the distribution of the second phases is not uniform. After T6 treatment, certain amount of MgZn2 was precipitated along the grain boundary which deteriorates the corrosion resistance. The second phase in as-cast is more concentrated than the others. So its corrosion resistance is better than T6 treated sample whose second phase is distributed everywhere along the grain boundary.

(2) T5 treated alloy has the best corrosion resistance exhibiting uniform corrosion. The alloys are mainly corroded by pitting corrosion especially the as-extruded and T6 treated samples are severely corroded. Although the as-cast alloy is corroded by pitting corrosion, it shows good corrosion resistance compared with the as-extruded and T6 treated. The corrosion resistance of the four states of ZK60 can be ranked as following: T5 treated > as-cast > T6 treated > as-extruded.

Acknowledgement

This work was supported by the National Basic Research Program of China (973 Program) (No. 2012CB619101), National Natural Science Foundation of China (No.81401773) and National High Technology Research and Development Program of China (863 Program, No.2015AA033701).

References

[1] M.P. Staiger, A.M. Pietak, J. Huadmai, G. Dias, Magnesium and its alloys as orthopedic biomaterials: a review, Biomaterials 27 (2006) 1728–1734.
[2] Y.L. Zhou, D.M. Luo, W.Y. Hu, Y.C. Li, P. Hodgson, C. Wen, Compressive

properties of hot-rolled Mg-Zr-Ca alloys for biomedical applications, Adv. Mater. Res. Switz 197–198 (2011) 56–59.
[3] Y. Sun, B. Zhang, Y. Wang, L. Geng, X. Jiao, Preparation and characterization of a new biomedical Mg–Zn–Ca alloy, Mater. Des. 34 (2012) 58–64.
[4] Y. Shi, M. Qi, Y. Chen, P. Shi, MAO-DCPD composite coating on Mg alloy for degradable implant applications, Mater. Lett. 65 (2011) 2201–2204.
[5] K.Y. Chiu, M.H. Wong, F.T. Cheng, H.C. Man, Characterization and corrosion studies of fluoride conversion coating on degradable Mg implants, Surf. Coat. Tech. 202 (2007) 590–598.
[6] F. Witte, V. Kaese, H. Haferkamp, E. Switzer, A. Meyer-Lindenberg, C.J. Wirth, et al., In vivo corrosion of four magnesium alloys and the associated bone response, Biomaterials 26 (2005) 3557–3563.
[7] T. Kraus, S.F. Fischerauer, A.C. Hanzi, P.J. Uggowitzer, J.F. Loffler, A.M. Weinberg, Magnesium alloys for temporary implants in osteosynthesis: in vivo studies of their degradation and interaction with bone, Acta Biomater. 8 (2012) 1230–1238.
[8] P. Zhou, H.R. Gong, Phase stability, mechanical property, and electronic structure of an Mg-Ca system, J. Mech. Behav. Biomed. 8 (2012) 154–164.
[9] Y.F. Ding, C.E. Wen, P. Hodgson, Y.C. Li, Effects of alloying elements on the corrosion behavior and biocompatibility of biodegradable magnesium alloys: a review, J. Mater Chem. B 2 (2014) 1912–1933.
[10] G. Mani, M.D. Feldman, D. Patel, C.M. Agrawal, Coronary stents: a materials perspective, Biomaterials 28 (2007) 1689–1710.
[11] N. Li, Y.F. Zheng, Novel magnesium alloys developed for biomedical application: a review, J. Mater. Sci. Technol. 29 (2013) 489–502.
[12] Z. Su, C. Liu, Y. Wan, Microstructures and mechanical properties of high performance Mg–4Y–2.4Nd–0.2Zn–0.4Zr alloy, Mater. Des. 45 (2013) 466–472.
[13] X. Zhang, G. Yuan, L. Mao, J. Niu, P. Fu, W. Ding, Effects of extrusion and heat treatment on the mechanical properties and biocorrosion behaviors of a Mg-Nd-Zn-Zr alloy, J. Mech. Behav. Biomed. Mater. 7 (2012) 77–86.
[14] X. Lin, L.L. Tan, Q. Zhang, K. Yang, Z.Q. Hu, J.H. Qiu, et al., The in vitro degradation process and biocompatibility of a ZK60 magnesium alloy with a forsterite-containing micro-arc oxidation coating, Acta Biomater. 9 (2013) 8631–8642.
[15] Y. Zong, G. Yuan, X. Zhang, L. Mao, J. Niu, W. Ding, Comparison of biodegradable behaviors of AZ31 and Mg–Nd–Zn–Zr alloys in Hank's physiological solution, Mater. Sci. Eng. B 177 (2012) 395–401.
[16] H.X. Yu, Effects of Li content on microstructure and corrosion morphology of Mg-Li-Al-Ca alloy in NaCl solution, in: Proceedings of the 2014 International Conference on Materials Science and Energy Engineering (Cmsee 2014), 2015, pp. 327–331.
[17] S.H. Cai, T. Lei, N.F. Li, F.F. Feng, Effects of Zn on microstructure, mechanical properties and corrosion behavior of Mg-Zn alloys, Mat. Sci. Eng. C Mater 32 (2012) 2570–2577.
[18] C.J. Boehlert, K. Knittel, The microstructure, tensile properties, and creep behavior of Mg–Zn alloys containing 0–4.4wt.% Zn, Mater. Sci. Eng. A 417 (2006) 315–321.
[19] E. Aghion, G. Levy, The effect of Ca on the in vitro corrosion performance of biodegradable Mg-Nd-Y-Zr alloy, J. Mater. Sci. 45 (2010) 3096–3101.
[20] Y. Zheng, Magnesium Alloys as Degradable Biomaterials, CRC Press, 2015.
[21] Z. Shi, M. Liu, A. Atrens, Measurement of the corrosion rate of magnesium alloys using Tafel extrapolation, Corros. Sci. 52 (2010) 579–588.
[22] H. Li, Q.M. Peng, X.J. Li, K. Li, Z.S. Han, D.Q. Fang, Microstructures, mechanical and cytocompatibility of degradable Mg-Zn based orthopedic biomaterials, Mater. Des. 58 (2014) 43–51.
[23] M. Yamasaki, N. Hayashi, S. Izumi, Y. Kawamura, Corrosion behavior of rapidly solidified Mg-Zn-rare earth element alloys in NaCl solution, Corros. Sci. 49 (2007) 255–262.
[24] G.L. Song, A. Atrens, M. Dargusch, Influence of microstructure on the corrosion of diecast AZ91D, Corros. Sci. 41 (1999) 249–273.
[25] A. Zomorodian, M.P. Garcia, T.M.E. Silva, J.C.S. Fernandes, M.H. Fernandes, M.F. Montemor, Biofunctional composite coating architectures based on polycaprolactone and nanohydroxyapatite for controlled corrosion activity and enhanced biocompatibility of magnesium AZ31 alloy, Mat. Sci. Eng. C Mater 48 (2015) 434–443.
[26] Y.L. Zhou, Y.C. Li, D.M. Luo, Effects of Nd on the microstructures, mechanical properties and in vitro corrosion behavior of cast Mg-1Mn-2Zn-xNd alloys, Mater. Trans. 56 (2015) 253–258.
[27] G.L. Song, A. Atrens, Understanding magnesium corrosion - a framework for improved alloy performance, Adv. Eng. Mater. 5 (2003) 837–858.
[28] R.C. Zeng, L. Sun, Y.F. Zheng, H.Z. Cui, E.H. Han, Corrosion and characterisation of dual phase Mg-Li-Ca alloy in Hank's solution: the influence of microstructural features, Corros. Sci. 79 (2014) 69–82.